Journal of Engineering Mathematics **26**: 509–524, 1992.

A mathematical model and numerical estimation of setting stresses in polymer composites molded under hydrostatic pressure

A.M. BORIEK[1], A.S. EL-BAKRY[2] and C.D. ARMENIADES[3]

Departments of [1]Mechanical Engineering and Materials Science; [2]Mathematical Sciences; [3]Chemical Engineering; Rice University, P.O. Box 1892, Houston, TX 77251-1892, USA

Received 12 September 1991; accepted in revised form 23 March 1992

Abstract. The effect of compression molding (i.e. molding under hydrostatic pressure) on the magnitude and distribution of setting stresses in particle-reinforced polymer composites is investigated using the finite element method. Models based on fairly random arrangements of the reinforcing particles are used, with different particle size gradations, as well as different aggregate-to-resin ratios. An analytical expression of the maximum setting stresses in these composites is introduced. A non-linear constrained optimization technique is used to obtain the mathematical model parameters which aid in a reasonable numerical estimation of the maximum setting stresses in real systems. The numerical results show that externally applied hydrostatic pressure helps diminish some of the local setting stresses. However, this relief becomes insignificant at the interface between aggregate particles and the resin domains where local setting stresses are maximum. This indicates that the practice of compression molding does not have a significant effect in reducing local setting stresses in ordinary polymer concrete systems.

1. Introduction

Various types of polymer concrete (PC), a composite consisting of mineral aggregate (sand and gravel) and an organic resin binder that hardens of polymerization, are finding increasing use in load-bearing structures. These composites suffer from setting stresses, generated during the curing process due to shrinkage of the polymerizing resin (cure shrinkage), as the secondary bonds with distances of 3–5 Å between monomer molecules are converted into primary, covalent bonds with distances of ca. 1.5 Å in the polymer chain network. Since PC systems contain particulate reinforcement up to 80% by volume, the resin binder is largely confined to the interstices between the aggregate particles. When the resin starts to polymerize, a small amount of cure shrinkage brings these particles in contact, thus forcing the resin to complete its cure in constant-volume domains. This inhibition of polymerization shrinkage generates a field of tensile stresses, the "setting stresses". Cure shrinkage and the resulting setting stresses are both highly undesirable. Poor control of cure shrinkage impairs the moldability, dimensional stability, and appearance of the cured composite. Setting stresses decrease its strength and significantly impair its creep resistance.

Since the setting stresses are tensile in nature, there is a traditional belief in the plastics industry that compression molding (i.e. curing the composite under hydrostatic pressure) is an effective means of alleviating setting stresses. In this paper we utilize a model, previously developed for estimating setting stresses in particle reinforced polymer composites, to study the effect of compression molding on the magnitude and distribution of local setting stresses.

In a series of recent publications [1–4] we presented several three-dimensional finite element models, which predict the location, magnitude, and distribution of setting stresses, given the cure shrinkage and physical properties of the resin binder, and the size distribution

of the reinforcing particles. These models ranged from systems with orderly arrangements of spherical aggregate particles to systems based on fairly random arrangements of nonspherical particles. In particular the "FRA" model, based on a fairly random arrangement of quasi-spherical and quasi-ellipsoidal particles, gives a very realistic representation of the actual composites, since it describes accurately the shape of the aggregate particles used in polymer concrete as well as the packing arrangement of these particles in the composite. The criteria used in constructing this model are: (a) the particles are quasi-spherical or quasi-ellipsoidal in shape, (b) they occupy more than 50% of the space with the largest particles touching each other, and (c) for systems with relatively high packing factors,[†] the particle sizes range over one order of magnitude [5].

The results of extensive numerical experiments using finite element analysis (FEA) of these models have led to the development of a mathematical expression, which gives the functional dependence of the maximum principal setting stresses on the material and geometric parameters of the composite in the absence of any applied hydrostatic pressure. This equation was presented in [4]. We discuss briefly some of its subsidiary functional dependencies. It was found that as the percentage of inherent shrinkage increases, the setting stresses tend to increase linearly. The Poisson's ratios of the resin material vary linearly with the logarithmic value of the maximum principal stresses. Moreover, the Poisson's ratio of the aggregate particles were found to have a negligible effect on setting stresses. It was also shown that the maximum principal stresses vary linearly with resin to aggregate volume ratio in the composite. These numerical experiments were performed on a wide range of models. These models include several three-dimensional finite element models of orderly arrangement of single [1] and multiple sized spherical reinforcing particles [2] as well as the FRA models. It was also found that a third order polynomial was the best fit for the relationship between the maximum setting stresses and the aggregate-to-resin Young's modulus ratio over a realistic range of materials properties of the individual phases in these models. The mathematical expression is stated as follows:

$$\sigma_{\max} = \zeta \, e^{\nu} V(g(\alpha), S_w) \sum_{k=0}^{3} \psi_k(g(\alpha), S_w) \beta^k , \tag{1}$$

where

$\sigma_{\max}$ = maximum principal tensile setting stress in the PC, normalized with respect to the tensile strength of the composite.

$\psi_k(g(\alpha), S_w)$ = coefficient functions depending on size distribution (α), geometric arrangement (g) and shape of the aggregate particles; S_w (where S_w is the weighted average of S_i, the ratio of the minor to major axes of aggregate particles).

ν = Poisson's ratio of the cured resin.

ζ = inherent shrinkage of the resin (in volume %).

$V(g(\alpha), S_w)$ = resin to aggregate volume ratio in the composite. This ratio is uniquely defied for each geometric arrangement and size distribution of a given shape of aggregate particles.

β = logarithmic value of the ratio of the tensile (Young's) moduli of aggregate and resin; $\beta > 0$.

[†] The packing factor is equal to the total volume of the solid particles divided by the total volume of the composite.

In this study we use nonlinear constrained optimization techniques to compute the values of the unknown parameters in the mathematical model. Several equivalent formulations of the mathematical model are presented. Different techniques are used to solve the problem which give rise to different solutions. The technique that best fits the physical considerations of the problem is presented last and used to compute the coefficient functions of the mathematical model. We then use finite element analysis to estimate the maximum setting stresses in polymer composites reinforced with quasi-spherical, and/or quasi-ellipsoidal particles and molded under hydrostatic pressure.

2. Composite models

Our composite models contain quasi-spherical and quasi-ellipsoidal particles ranging within the ASTM C33 standards of size gradation [6]; these particles are packed in arrangements that are almost random but retain some rudimentary spatial order in that smaller particles usually occupy the spaces between the larger particles. We call this model the fairly random arrangement (FRA). The symmetric boundary conditions that are applied to these models force the resin to shrink in constant volume domains so that the required field of stress is generated in the entire composite.

Following the technique used in our previous studies [1–4] we have simulated the setting stresses and resulting strains in the cured composites by means of a thermal shrinkage model, in which the resin (with an assumed bulk thermal expansion coefficient, $\alpha = 2.58 \times 10^{-4}\,°C^{-1}$) shrinks against a thermally invariant aggregate ($\alpha = 0.0$). This generates in the resin domains tensile stresses, which simulate the setting stresses. Hydrostatic pressure is applied to the boundaries of the FRA models, superimposing compressive stresses. This study examines the magnitude and location of the maximum setting stresses generated in the

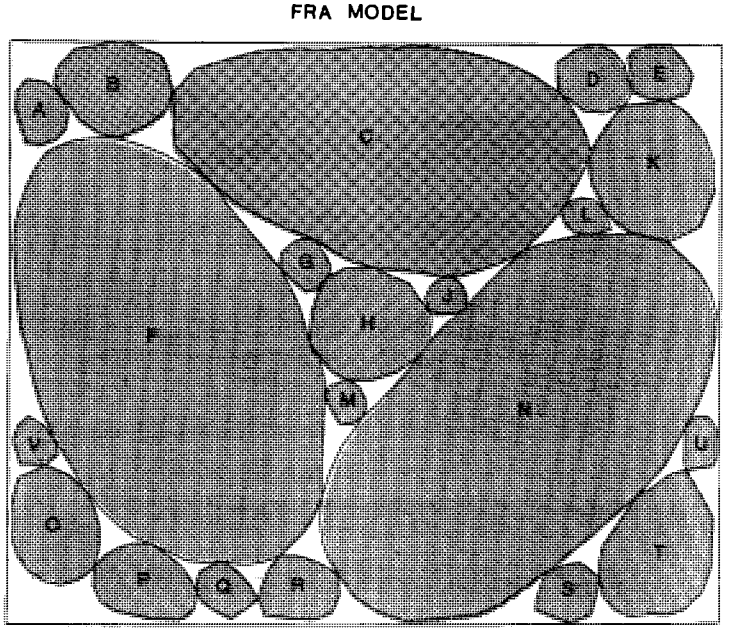

Fig. 1. Fairly random arrangement of void/aggregate domains.

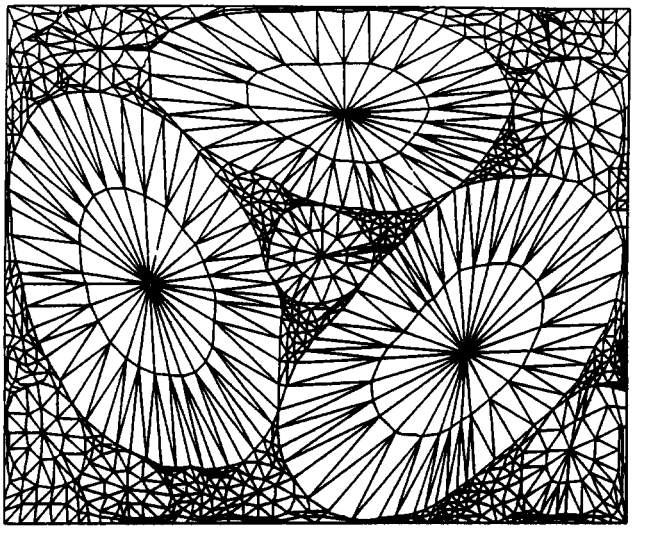

Fig. 2. Finite element network of the FRA model (1565 elements and 4015 nodes).

presence of the applied pressure. The stresses are computed using the PAFEC finite element program [7, 8].

An exemplar FRA model is shown in Fig. 1 in the form of a representative volume element. This element contains all of the variations in size, shape and organization of the reinforcing particles, hence it represents a random cross section through the actual composite. It is noteworthy that the fact that representative volume element boundaries do not intersect any particles allows us to apply symmetric boundary conditions without creating particles with unrealistic shapes.

2.1. Finite element analysis

Figure 2 shows a finite element network of 1656 finite isoparametric elements and 4015 nodes, formed for the unit cell of the FRA example shown in Fig. 1. A plane strain analysis is considered. Planes of symmetry pass through the boundaries of the FRA models. These symmetric planes ensure that the resin shrinks at constant volume domains. The stresses generated by the applied pressure are nonuniformly distributed throughout the composite. The tensile setting stresses are also nonuniform in their distribution since we have a heterogeneous material. The FEA results show the location and magnitude of maximum stresses in the various models cured under applied hydrostatic pressure.

3. Mathematical model

The numerical estimation of maximum setting stresses depends on the availability of material parameters such as the elastic moduli and Poisson's ratio for the different constituents of the composite, and the inherent cure shrinkage of the resin. The composite is assumed to be macroscopically isotropic. According to this assumption the material properties of the constituents are to be invariant from point to point within the composite. Both resin and

aggregate are assumed to respond elastically to the generated setting stresses. It is assumed that aggregate-to-resin adhesion exceeds the cohesive strength of the cured resin. Cure-shrinkage forces within the resin are isotropic and develop uniformly throughout the composite under an applied hydrostatic pressure. We have ignored any thermal stresses generated by temperature changes during resin cure. This assumption is quite reasonable for polymer concrete systems, cured at ambient temperatures. In these systems the inert mineral aggregate comprises 70–85% of the volume and, because of its higher density, up to 90% of the total mass of the composite. Consequently, the exotherm generated by the polymerization of the resin binder does not increase appreciably the temperature of the overall composite during its cure.

The numerical results of our finite element analysis of several FRA models under applied hydrostatic pressure show that the effect of hydrostatic pressure on the maximum principal stresses in a particle-reinforced composite can be included in equation (1) as follows:

$$\sigma_{\max} = (1 - P_{\text{rel}})\zeta\, e^{\nu} V(g(\alpha), S_w) \sum_{k=0}^{3} \psi_k(g(\alpha), S_w)\beta^k , \tag{2}$$

where P_{rel} is a dimensionless pressure term obtained by normalizing the externally applied pressure with respect to the tensile strength of the composite in the absence of setting stresses. For example, in specially formulated PC systems[†] containing 75% by volume mineral aggregate in polyester/styrene matrix, the measured splitting tensile strength[‡] was 7.13×10^6 N/m^2. Equation (2) is applicable only to void-free systems.[**]

4. Numerical experiments

Extensive numerical experiments were performed using PAFEC to obtain the maximum principal stresses σ_i, $i = 1, \ldots, n$. A set of observations for the physical parameters: ν_i, β_i, ζ_i, $i = 1, \ldots, n$ were chosen within realistic ranges of values for the materials properties of the composite. These are ν: 0.30–0.37, ζ: 0.1–0.21, β: 0.43–2.8399, and P_{rel}: 0.0–1.547, where P_{rel} is the applied hydrostatic pressure normalized against tensile strength of the stress-free composite. These observations are substituted in the mathematical expression (2) to obtain a system of linear equations with the model parameters $\psi_k(g(\alpha), S_w)$ as unknowns. The linear system has the form $\mathbf{A}\boldsymbol{\psi} = \mathbf{y}$. The entries of the matrix $\mathbf{A}$, the vector $\boldsymbol{\psi}$, and the vector $\mathbf{y}$ are defined as follows:

$$\mathbf{A} = (a_{ij}) , \qquad a_{ij} = p_i\, e^{\nu_i}\zeta_i V_i \beta_i^{j-1} , \quad j = 1, \ldots, k, \; i = 1, \ldots, n , \tag{4a}$$

$$\boldsymbol{\psi}(g(\alpha), S_w) = (\psi_k(g(\alpha), S_w)) , \quad k = 0, 1, 2, 3 , \tag{4b}$$

[†] In these systems, setting stresses were eliminated by the addition of carefully measured amounts of a chemical agent, which expands during resin cure thus counteracting polymerization shrinkage [9].

[‡] The splitting tensile measurements were performed on cylindrical specimens according to the ASTM C-116 standards using 7.62 cm diameter by 10.16 cm long specimens. The cylinders were subjected to transverse crushing loads at a cross-head speed of 0.01 in/min. The splitting tensile strength S is given by $S = 2P_f/3.14DL$, where P_f is the load at fracture, D and L are the diameter and length of the specimen respectively [9].

[**] These systems are assumed to be void-free since the externally imposed pressure during their cure is expected to expel any air bubbles entrained into the uncured system.

$$\mathbf{y} = (\sigma_{\max_j}), \quad j = 1, \ldots, n. \tag{4c}$$

The least-squares technique can be used to obtain the vector of the unknown model parameters; $\psi_k(g(\alpha), S_w)$. However, the solution may yield non-physical answers for the magnitude of maximum setting stresses. We discuss this in the next section.

4.1. Constrained least-squares formulation

The maximum tensile setting stress component σ_i is nonnegative. It is also clear that e^{ν_i}, $V_i(g(\alpha), S_w)$, and, ζ_i, $i = 1, \ldots, n$ are all positive. For this reason we impose a nonnegativity constraint on the summation term in equation (2) in order to ensure a physically meaningful prediction of the magnitude of maximum tensile setting stresses.

The least-squares formulation for our problem can be stated as follows:

$$\underset{\boldsymbol{\psi}(g(\alpha),S_w)\in\mathbf{R}^k}{\text{minimize}} \; \|\mathbf{A}\boldsymbol{\psi}(g(\alpha), S_w) - \mathbf{y}\|_2, \tag{4.1a}$$

where

$$\mathbf{A} \in \mathbf{R}^{n\times k}, \quad \mathbf{y} \in \mathbf{R}^n, \tag{4.1b}$$

$$\|\mathbf{A}\boldsymbol{\psi}(g(\alpha), S_w) - \mathbf{y}\|_2 = \|\mathbf{r}\|_2, \tag{4.1c}$$

is the Euclidean vector norm defined by $\|r\|_2 = \sqrt{\left(\sum_{i=1}^{n} r_i^2\right)}$. Equation (4.1a) represents a linear least squares problem and $\boldsymbol{\psi}$ which solves (4.1a) is the least squares solution of the system $\mathbf{A}\boldsymbol{\psi}(g(\alpha), S_w) = \mathbf{y}$.

The following constrained least-squares formulation.

$$\underset{\boldsymbol{\psi}(g(\alpha),S_w)\in\mathbf{R}^k}{\text{minimize}} \; \|\mathbf{A}\boldsymbol{\psi}(g(\alpha), S_w) - \mathbf{y}\|_2 \tag{4.1.1a}$$

subject to

$$\mathbf{B}\boldsymbol{\psi}(g(\alpha), S_w) \geqslant 0, \tag{4.1.1b}$$

where

$$\mathbf{B} = (b_{ij}), \qquad b_{ij} = \beta_i^j, \quad i = 1, \ldots, n, \; j = 1, \ldots, k. \tag{4.1.1c}$$

Problem (4.1.1) has a non-differentiable objective function. This is a drawback since special methods are needed to deal with the nondifferentiability. Consequently, we loose the advantage of widely used well-developed algorithms that require differentiability. For this reason, we consider an equivalent formulation to problem (4.2), namely the quadratic programming formulation (QPF).

4.2. Quadratic programming formulation

The QPF of our problem can be stated in the following form:

$$\underset{\psi(g(\alpha),S_w)\in\mathbf{R}^k}{\text{minimize}}\ \mathbf{b}^T\psi(g(\alpha),S_w)+\frac{1}{2}\,\psi(g(\alpha),S_w)^T\mathbf{Q}\psi(g(\alpha),S_w)\,, \tag{4.2a}$$

subject to

$$\mathbf{B}\psi(g(\alpha),S_w)\geq 0\,, \tag{4.2b}$$

where

$$\mathbf{b}=-2\mathbf{A}^T\mathbf{y}\,, \tag{4.2c}$$

$$\mathbf{Q}=2\mathbf{A}^T\mathbf{A}\,. \tag{4.2d}$$

If $\mathbf{A}$ has k linearly independent columns (i.e. $\mathbf{A}$ has full column rank), then the matrix $\mathbf{A}^T\mathbf{A}$ is positive definite. In general, $\mathbf{A}$ may not have full column rank, consequently, the Hessian matrix $\mathbf{Q}$ will not be positive definite. However, $\mathbf{Q}$ is at least positive semi-definite.[†] The QPF consists of a convex quadratic objective function which is minimized over the feasible set $\mathbf{S}=\{\psi:\mathbf{B}\psi\geq 0\}$.

As is well-known in the case of convex programming, each local solution is a global one. Unfortunately, the solution to our problem may not be unique since in general, the objective function is not strictly convex. A modification of the objective function (4.2a) is needed to force the uniqueness of the solution on our problem. The Hessian matrix has to perturbed to force the positive definiteness property.[‡] This can be accomplished by adding a small perturbation ε to the diagonal entries of the Hessian. This technique is presented in the following modified quadratic programming formulation (MQPF):

4.3. Modified quadratic programming formulation

The MQPF can be stated as follows:

$$\underset{\psi(g(\alpha),S_w)\in\mathbf{R}^k}{\text{minimize}}\ \mathbf{b}^T\psi(g(\alpha),S_w)+\frac{1}{2}\,\psi(g(\alpha),S_w)^T(\mathbf{Q}+\varepsilon\mathbf{I})\psi(g(\alpha),S_w)\,, \tag{4.3a}$$

subject to

$$\mathbf{B}\psi(g(\alpha),S_w)\geq 0\,. \tag{4.3b}$$

In (4.3a), if ε is chosen properly, the MQPF would consist of a strictly convex quadratic objective function. This function is minimized over the feasible set $\{\psi(g(\alpha),S_w):\mathbf{B}\psi(g(\alpha),S_w)\geq 0\}$. In order to prove the existence of the solution to problem (4.3) one has to consider only the constraints that are relevant to this problem. These constraints are the ones that are active at the solution $\psi^*(g(\alpha),S_w)$ (Appendix A.1). Let $\mathbf{B}_{\text{active}}$ be the sub-matrix of $\mathbf{B}$ that is corresponding to such constraints. Hence, problem (4.4) is reduced to the following equality constrained optimization problem:

[†] Since $\mathbf{Q}=\mathbf{A}^T\mathbf{A}$, then, $\psi^T\mathbf{Q}\psi=\psi^T\mathbf{A}^T\mathbf{A}\psi=\|A\psi\|_2^2\geq 0$.

[‡] The positive definiteness of the Hessian of the objective function guarantees the existence of a unique solution.

$$\underset{\psi(g(\alpha),S_w)\in\mathbf{R}^k}{\text{minimize}}\ q(\psi(g(\alpha),S_w))\,, \tag{4.3c}$$

subject to

$$\psi(g(\alpha),S_w)\in\mathbf{S}\,, \tag{4.3d}$$

where

$$q=\mathbf{b}^T\psi(g(\alpha),S_w)+\frac{1}{2}\,\psi(g(\alpha),S_w)^T(\mathbf{Q}+\varepsilon\mathbf{I})\psi(g(\alpha),S_w) \tag{4.3e}$$

and

$$\mathbf{S}=\{\psi(g(\alpha),S_w)\colon \mathbf{B}_{\text{active}}\psi(g(\alpha),S_w)=0\}\,. \tag{4.3f}$$

The objective function q is continuous, convex, and weakly coercive (i.e. satisfies the property $q(\psi(g(\alpha),S_w))\to+\infty$ as $\|\psi(g(\alpha),S_w)\|\to\infty$ (Appendix A.2)). The feasible set $\mathbf{S}$ is closed and convex (since $\mathbf{S}$ is a subspace of $\mathbf{R}^k$). These properties of both q and $\mathbf{S}$ ensure the existence of the solution of problem (4.3) [10, 11].

In order to study the behavior of ε in problem (4.3), one has to consider an equivalent formulation using the model trust-region strategy. This strategy is one of the most successful globalization techniques in constrained optimization. The main idea of this strategy is to add a ball constraint which restricts the size of the step taken by the algorithm [12]. The new equivalent problem is called trust-region quadratic programming (TRQP). It can be stated as follows:

$$\underset{\psi(g(\alpha),S_w)\in\mathbf{R}^k}{\text{minimize}}\ \mathbf{b}^T\psi(g(\alpha),S_w)+\frac{1}{2}\,\psi(g(\alpha),S_w)^T\mathbf{Q}\psi(g(\alpha),S_w)\,, \tag{4.3.1a}$$

subject to

$$\mathbf{B}\psi(g(\alpha),S_w)\geq 0\,, \tag{4.3.1b}$$

$$\|\psi(g(\alpha),S_w)\|_2\leq\delta\,, \tag{4.3.1c}$$

where $\|\cdot\|_2$ designate the l_2 norm and δ is a positive constant represents the radius of the trust region, which depends on ε.[†] In the formulation of problem (4.4), the choice of ε affects the behavior of the solution. Very large values of ε cause the problem to be ill-conditioned, which would decrease the accuracy of the numerical solution. It may also result in an inconsistency of the hyperplane (4.3.1b) determined by the active constraints (Appendix A.1) and the trust region ball (4.3.1c). Consequently, the feasible region will be empty. However, the value of ε has to be chosen sufficiently large that the Hessian matrix is safely positive definite [3].

[†] Large values of ε is an indication that the radius of the trust region δ is small and vice versa.

5. Results and discussion

The QPSOL is used to compute the mathematical model parameters $\psi(g(\alpha), S_w)$ (Appendix A.3). Table 1 shows the computed values of $\psi_k(g(\alpha), S_w)$ for different PC systems reinforced with fairly random arrangements of aggregate particles (FRA models). These models are for composites cured under hydrostatic pressure. These composites differ from each other in terms of the inherent cure shrinkage of their resin matrix, the respective moduli of resin and reinforcing particles, the geometric shape of these particles, and their size distribution.

The $\psi_k(g(\alpha), S_w)$ values can be used to calculate the magnitude of the maximum setting stresses in these systems under the assumptions stated in Section 3. The formulation can be applied to any PC system reinforced with spherical or quasi-spherical aggregate particles. The packing factor,* size distribution, shape, and geometric arrangement of the reinforcing particles uniquely determine values for $\psi_k(g(\alpha), S_w)$ for a particular PC system. We note

Table 1. Characteristics of the FRA models

Model	Aggregate domains†	$V_{\text{resin/aggregate}}$	Packing factor	$\psi(g(\alpha), S_w)$‡
FRA-86	A through U	0.1573	86.406	0.9582600007D + 01 0.0000000000D + 00 0.9488875027D + 01 −0.3613427658D + 01
FRA-82	A, B, C, D, E, F, N, V, O, Q, R, S, T, U, G, J, M, H, P	0.2195	82.001	0.7509721461D + 01 0.0000000000D + 00 0.7078096698D + 01 −0.2647384458D + 01
FRA-78	B, C, N, F, O, T, K, H	0.282	78.003	0.7657477360D + 01 0.0000000000D + 00 0.88914951090D + 01 −0.3346498818D + 01
FRA-71	C, F, H, N, K	0.4083	71.006	0.5969345333D + 01 0.0000000000D + 00 0.2652011535D + 01 −0.7436865814D + 00
FRA-69	C, F, G, J, M, N, K	0.449	69.011	0.5655753152D + 01 0.0000000000D + 00 0.1919986584D + 01 0.0000000000D + 00
FRA-65	C, F, N	0.5383	65.007	0.5269824012D + 01 0.0000000000D + 00 0.8663340591D + 00 −0.5351225743D − 01

† Letters specifying aggregate domains are shown in Fig. 1.

‡ These values were computed using specified ranges of the materials properties: ν: 0.30–0.37; ζ: 0.1–0.21, β: 0.43–2.8399, and P_{rel}: 0.0–1.547, where P_{rel} is the applied hydrostatic pressure normalized against tensile strength of the stress-free composite.

* Packing factor is the ratio of the volume of the reinforcing particles to the total volume of the composite.

that in all of the analyzed models the value of $\psi_1(g(\alpha), S_w)$ is zero. This indicates that $\psi_1\beta$ has no effect on the prediction of maximum setting stresses. Linear terms, however, may not vanish for other models.

Figures 3.1 through 3.6 show maximum setting stresses, normalized against the tensile strength of the stress-free composite and plotted against the rank of the maximum setting stresses at different locations in the resin domains. These data indicate that the effect of external pressure on setting stresses varies considerably from point to point, being most significant at points well within the resin domain. However, the setting stresses of these points (even in the absence of external pressure) are not the highest: maximum setting stresses occur at the interface between the resin and aggregate. At these points the effect of external pressure is not significant. For example, in FRA-86 an external pressure of 11 MPa (1600 psi) reduces the maximum setting stress (at nodal point of rank 1) by only 7.35% (from 0.337 to 0.3386) of the composite strength. This percent decrease in maximum setting stress varies among the different FRA models. However, it does not exceed 8.62% (in FRA82). The effects of external pressure on the maximum setting stress in the six FRA models are summarized in Fig. 4. It is noteworthy that the baseline stresses (in the absence of external pressure) vary greatly between models. Setting stresses are relatively small in FRA86 and FRA82 due to efficient packing and optimum aggregate size gradation; setting stresses are much higher in the other models with lower and less efficiently packed aggregate. However, the effect of imposed hydrostatic pressure in lowering maximum setting stresses is very small in all of these systems. Since failure initiates at the points with the highest stress, the results of this work open question as to the effectiveness of compression molding in reducing local setting stresses in polymer concrete systems.

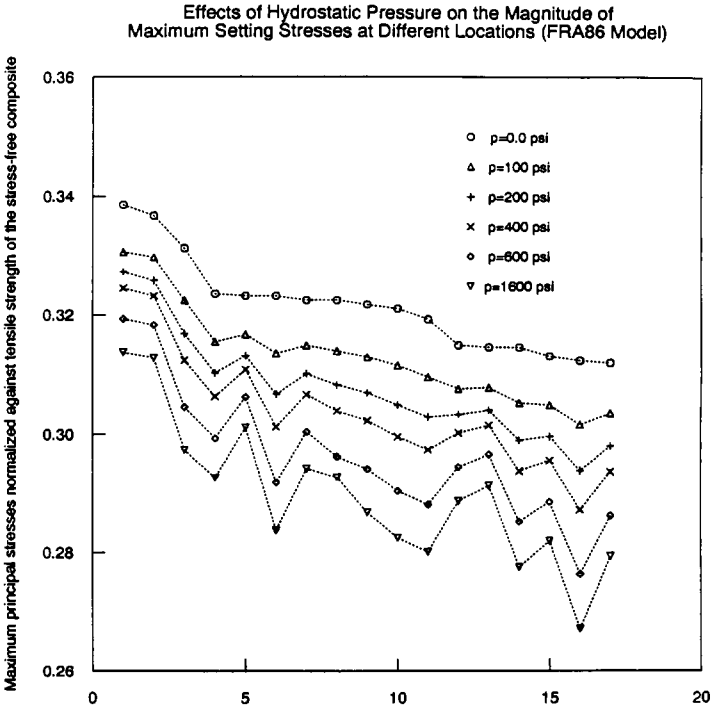

Fig. 3.1. Nodal points with the highest setting stresses under zero external pressure, ranked from left to right in order of decreasing setting stress.

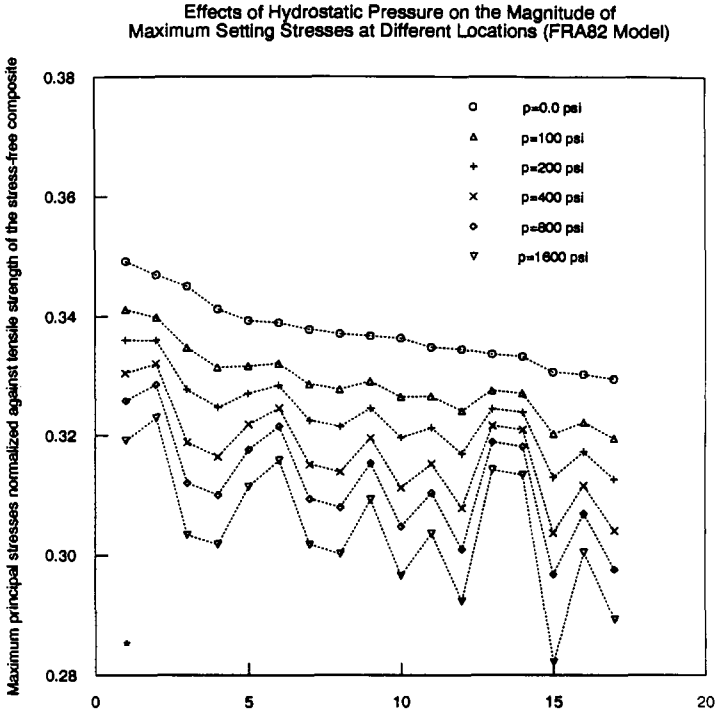

Fig. 3.2. Nodal points with the highest setting stresses under zero external pressure, ranked from left to right in order of decreasing setting stresses.

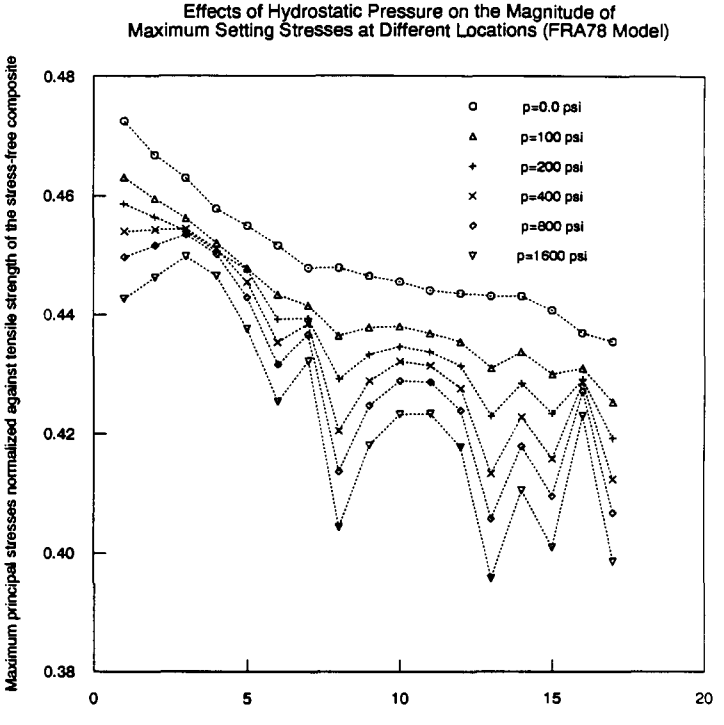

Fig. 3.3. Nodal points with the highest setting stresses under zero external pressure, ranked from left to right in order of decreasing setting stress.

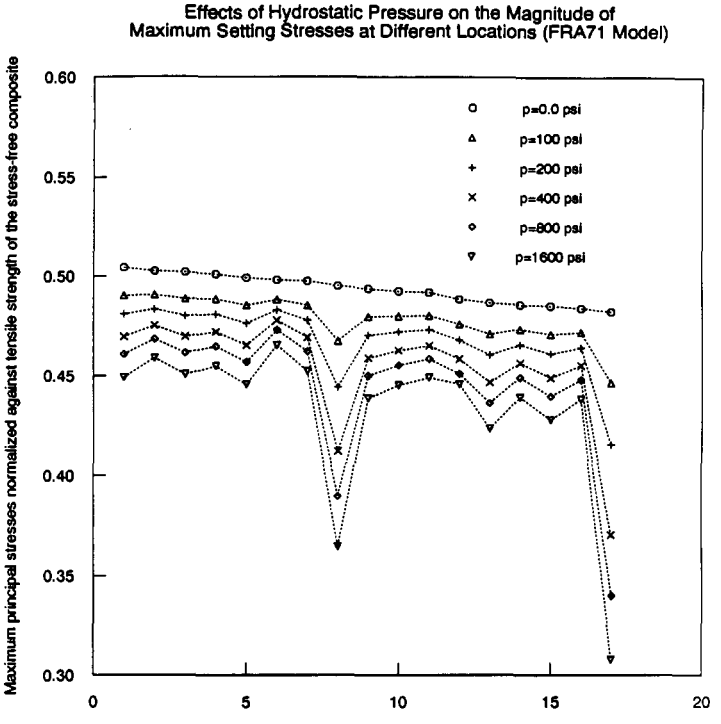

Fig. 3.4. Nodal points with the highest setting stresses under zero external pressure, ranked from left to right in order of decreasing setting stress.

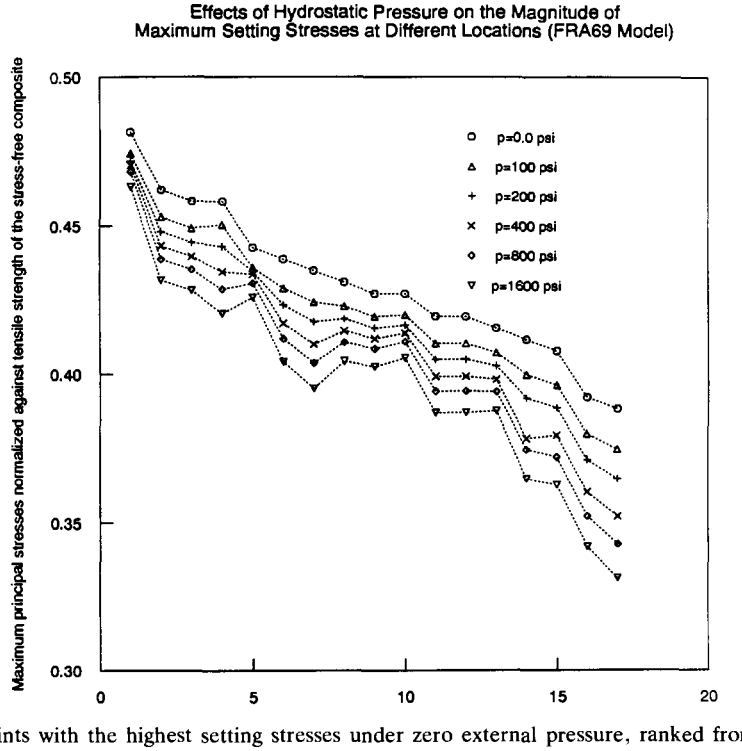

Fig. 3.5. Nodal points with the highest setting stresses under zero external pressure, ranked from left to right in order of decreasing setting stress.

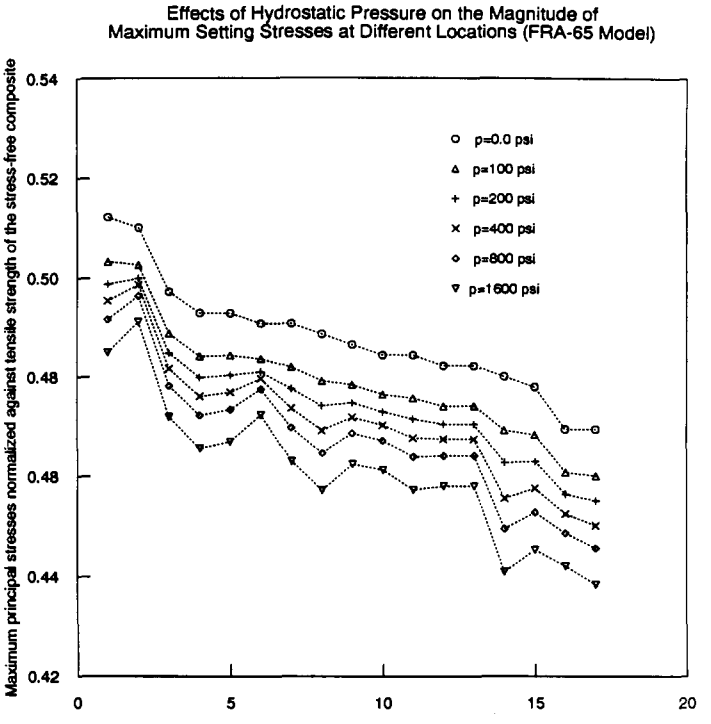

Fig. 3.6. Nodal points with the highest setting stresses under zero external pressure, ranked from left to right in order of decreasing setting stress.

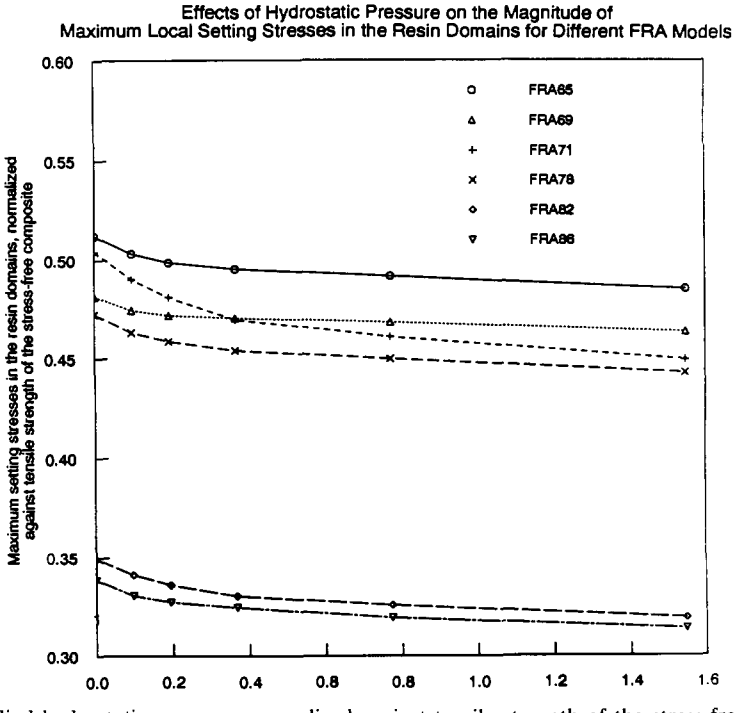

Fig. 4. Applied hydrostatic pressure, normalized against tensile strength of the stress-free composite.

6. Applications of models to real composites

Assuming that the magnitude of applied pressure, volume ratio of resin to aggregate, the size distribution and shape of the aggregate particles, and the material properties of the resin (Poisson's ratio, modulus of elasticity and inherent shrinkage of the resin) are known, one can determine which model comes closest to the actual composite so the proper choice of the values $\psi_k(g(\alpha), S_w)$, $k = 0, 1, 2, 3$ can be made. These values are dependent only on the geometric arrangement, size distribution and shape of the reinforcing particles. For example, assume that we have a PC system based on unsaturated polyester/styrene and reinforced with Ottawa sand, which is quasispherical. Assume also that the volume fraction of the aggregate in this system is 86% and that the size distribution of the particles falls within the ASTM C33 standard system. For a system with the previous characteristics the maximum setting stresses is estimated according to the developed formulation to be 33.86% of the splitting tensile strength of the composite. This is in the absence of the applied hydrostatic pressure. This percentage becomes slightly smaller when hydrostatic pressure is taken into account (32.14% for $p = 0.442$ of the splitting tensile strength of the composite). This can be used to estimate the maximum load that can be applied to the composite system before fracture for composites processed in the absence as well as under applied hydrostatic pressure.

7. Concluding remarks

Some reduction in setting stresses can be achieved by molding particle-reinforced composites under hydrostatic pressure. However, this reduction is not significant at locations where setting stresses are maximum, i.e. at the resin/particle interfaces. Since these locations are the primary candidates for initiation of microcracks that may cause failure, the practical importance of compression molding in reducing setting stresses is open to question. Analysis of different models of these composites show that the most effective means for lowering setting stresses is efficient packing and proper gradation of the reinforcing particles.

Appendix A

A.1. Inequality constraints

Consider the general nonlinear programming problem (NLP):

$$\text{minimize } f(x) \tag{A.1a}$$

subject to

$$c_i(x) = 0\,, \quad i = 1, \ldots, m\,, \tag{A.1b}$$

$$c_i(x) \geq 0\,, \quad i = m+1, \ldots, m+p\,. \tag{A.1c}$$

An inequality constraint $c_i(x) \geq 0$ is called *active* or *binding* at a feasible point x if it is

satisfied as equality at that point (i.e. $c_i(x) = 0$). An equality constraint is said to be active at any feasible point x. Let $A(x) = \{i: 1 \leq i \leq m \text{ or } c_i(x) = 0, i = m+1, \ldots, m+p\}$ denote the set of constraints that are active at the feasible point x of the nonlinear programming problem (NLP). If the set $A^* = A(x^*)$ (i.e. the set of constraints that are active at a solution x^* of problem (NLP) is known, the remaining inequality constraints can be deleted and the problem reduces to an equality constrained optimization problem [13, 14].

A.2. Weak coercivity of MQPF objective function

Consider the following quadratic function:

$$f(\mathbf{x}) = \mathbf{a}^T\mathbf{x} + \frac{1}{2}\mathbf{x}^T\mathbf{H}\mathbf{x}, \tag{A.2.1}$$

where

$$\mathbf{a} \in \mathbf{R}^k, \quad \mathbf{x} \in \mathbf{R}^k \quad \text{and} \quad \mathbf{H} \in \mathbf{R}^{k \times k}.$$

If $\mathbf{H}$ is positive definite, then $f(x) \to \infty$ as $\|\mathbf{x}\| \to \infty$.

Proof. Without loss of generality, we consider the function:[†]

$$\bar{f}(\bar{\mathbf{x}}) = \frac{1}{2}\bar{\mathbf{x}}^T\mathbf{H}\bar{\mathbf{x}} \tag{A.2.2}$$

Let $\lambda_1 \leq \lambda_2 \leq \cdots \leq \lambda_k$ be the eigenvalues of $\mathbf{H}$. It is known that for any Hermitian matrix $\mathbf{H}$, we have:

$$\lambda_1 = \min_{\bar{\mathbf{x}} \neq 0} \frac{\bar{\mathbf{x}}^T\mathbf{H}\bar{\mathbf{x}}}{\bar{\mathbf{x}}^T\bar{\mathbf{x}}} \tag{A.2.3}$$

$$= \min_{\bar{\mathbf{x}} \neq 0} \frac{\bar{\mathbf{x}}^T\mathbf{H}\bar{\mathbf{x}}}{\|\bar{\mathbf{x}}\|_2^2} \tag{A.2.4}$$

If $\mathbf{H}$ is positive definite, then,

$$\lambda_i > 0, \quad i = 1, \ldots, k, \tag{A.2.5}$$

and hence

$$\bar{\mathbf{x}}^T\mathbf{H}\bar{\mathbf{x}} \geq \lambda_1\|\bar{\mathbf{x}}\|_2^2 > 0, \quad \text{for all nonzero } \bar{\mathbf{x}} \in \mathbf{R}^k, \tag{A.2.6}$$

which shows that $\bar{f}(\bar{\mathbf{x}}) \to \infty$ as $\|\bar{\mathbf{x}}\|_2 \to \infty$.

A.3. QPSOL

The QPSOL is a set of subroutines which are designed to locate a minimizer of a quadratic function subject to linear constraints and simple upper and lower bounds on the variables

[†] Any function of the form (A.2.1) can be transformed to a function of the form (A.2.2) by transferring the coordinate axes to a point at which the linear term $\mathbf{a}^T\mathbf{x}$ vanishes.

[15]. If the quadratic function is strictly convex, a global minimizer is found; otherwise, a local minimizer is found.

The following is a general form of the QPF

$$\underset{\mathbf{x}\in\mathbf{R}^n}{\text{minimize}}\ \mathbf{c}^T\mathbf{x} + \frac{1}{2}\mathbf{x}^T\mathbf{H}\mathbf{x} \tag{A.3.1}$$

subject to

$$\mathbf{l} \leqslant \begin{Bmatrix} \mathbf{x} \\ \mathbf{A}\mathbf{x} \end{Bmatrix} \leqslant \mathbf{u}\,, \tag{A.3.2}$$

where $\mathbf{c}$ is a constant n-dimensional vector and $\mathbf{H}$ is a constant $n \times n$ symmetric matrix. $\mathbf{A}$ is an $m \times n$ matrix. $\mathbf{l}$ and $\mathbf{u}$ are constant n-dimensional vectors.

A subroutine for the formulation of the quadratic programming problem is developed. Different simulations are considered for each FRA model. For each simulation, ε is increased until a unique global minimizer is obtained.

Acknowledgement

We are indebted to the referees for their careful reading of this paper and their valuable suggestions for improving the paper.

This work is supported in part by Grant #DMR8713273 from the National Science Foundation. The second author is partially supported by the REDI foundation.

References

1. A.M. Boriek, J.E. Akin and C.D. Armeniades, Setting Stress Distribution in Particle Reinforced Polymer Composites, *Journal of Composite Materials*, 10 (1988) 986–1002.
2. A.M. Boriek, J.E. Akin and C.D. Armeniades, Setting Stress Distribution in Polymer Composites Reinforced with Multiple Sized-Aggregate, *Journal of ASCE, Materials Division*, 1 (1989) 217–236.
3. A.M. Boriek, M.M. El-Alem, J.E. Akin and C.D. Armeniades, A Theoretical Model for Voids Distribution in Polymer Composites and Their Effect on Setting Stresses, *Journal of Probabilistic Engineering Mechanics* 5 (3) (1990) 129–137.
4. A.M. Boriek, Modeling of Setting Stresses in Particle Reinforced Polymer Composites Using Finite Element Analysis, Ph.D. Thesis, Rice University (1989).
5. A.M. Boriek and C.D. Armeniades, Minimization of Setting Stresses Using Realistic Models for Particle Reinforced Polymer Composites, Presented in the Twenty-Third Annual Pittsburgh Conference on Modeling and Simulation, April 30–May 1, 1992.
6. *ASTM standards in building codes*, vol. II, American Society for Testing and Materials, ASTM, 1988.
7. R.D. Henshell, PAFEC 75 Theory, Results, PAFEC Ltd., Nottingham (1975).
8. *PAFEC Data Preparation Manual*, PAFEC Ltd., Nottingham, U.K. (1986).
9. E. Haque, Physicochemical Interaction between Montmorillonite and Polymerizing Systems: Effect on Particle-Reinforced Composites, Ph.D. Thesis, Rice University (1986).
10. A. Goldstein, Constructive Real Analysis, New York: Harper and Row (1967).
11. E. Zeidler, Nonlinear Functional Analysis and Its Applications, Vol. III, New York: Springer-Verlag (1984).
12. J.E. Dennis and R.B. Schnabel, Numerical methods for Unconstrained Optimization and Nonlinear Equations, Englewood Cliffs, NJ: Prentice-Hall, 129–133 (1983).
13. A.V. Fiacco and G.P. McCormick, Nonlinear Programming: Sequential Unconstrained Minimization Techniques, New York: John Wiley & Sons (1968).
14. R. Fletcher, Practical Methods of Optimization, New York: John Wiley & Sons (1987).
15. P.E. Gill, W. Murray, M.A. Saunders and M.H. Wright, *User's guide for QPSOL, a Fortran package for quadratic programming, version 3.2*, System Optimization Laboratory, Stanford University, CA, TR SOL 84-6, September (1984).